

CALIBRATION OF ANALYTICAL SOLUTION USING CENTRIFUGE MODEL TESTS ON MOORING LINES

by

S. Bang

South Dakota School of Mines and Technology, USA

R. J. Taylor

Naval Facilities Engineering Service Center, USA

H. Han

South Dakota School of Mines and Technology, USA

ABSTRACT

Single segmented mooring lines were tested in a geotechnical centrifuge for the purpose of calibrating the analytical solution developed for the analysis and design of various mooring lines associated with underwater drag/permanent anchors. The model mooring lines included steel ball chains and wire cables placed at various depths within the soft clayey seafloor soil. The mooring lines were loaded to preset tensions at the water surface under an elevated acceleration inside the centrifuge to simulate the field stress conditions experienced by the prototype mooring lines. This paper describes the calibration of two factors that are used as part of the input parameters in the analytical solution of mooring lines and considers the effect of chasing wires that were used in the experiment to determine the locations of the mooring lines.

KEY WORDS: Mooring line, centrifuge, soil bearing capacity factor, soil adhesion conversion factor.

INTRODUCTION

The U.S. Naval Facilities Engineering Service Center (NFESC) conducted a series of centrifuge model tests (Law, et. al, 1994) on buried mooring lines in order to validate the analytical model developed by Bang (1996). During the centrifuge model tests a set of chasing wires was attached to the mooring chains and cables. Figure - 1 shows a schematic sketch of the layout of the mooring line and chasing wires. The chasing wires were used to locate the exact geometries of the mooring chains/cable during transition from the initial to the final position due to the applied load.

However, it was found later that the chasing wires had a rather significant effect on the mooring line geometry and tension, particularly on the mooring cable because of its thin cross section. This paper studies the effect of the chasing wires on the performance of the mooring line and the soil in calibrating the material and geometric parameters necessary for the validation of the analytical model.

CENTRIFUGE MODEL TESTS

The primary objective of the centrifuge model tests was to obtain the detailed load transfer mechanism of the mooring line embedded in a cohesive seafloor. Therefore, the mooring lines were fixed at specific

depths. They were tested under a centrifugal acceleration equal to 80 times the gravitational acceleration in order to simulate the nonlinear stress-dependent behavior of the soil. The tests included three ball chains and one cable embedded at various depths to model the mooring lines in Speswhite kaolin, a white potter's clay (Dunnavant and Kwan, 1993). The model ball chain had a ball diameter of 0.48 cm and was loaded to 208.52 N, and the model cable had a diameter of 0.48 cm and was loaded to 231.3 N horizontally at the seafloor surface. Note that the corresponding prototype geometric dimensions become model dimensions multiplied by the applied centrifugal acceleration level as a multiple of the gravitational acceleration. However, the corresponding prototype load is obtained by multiplying a square of the applied acceleration level.

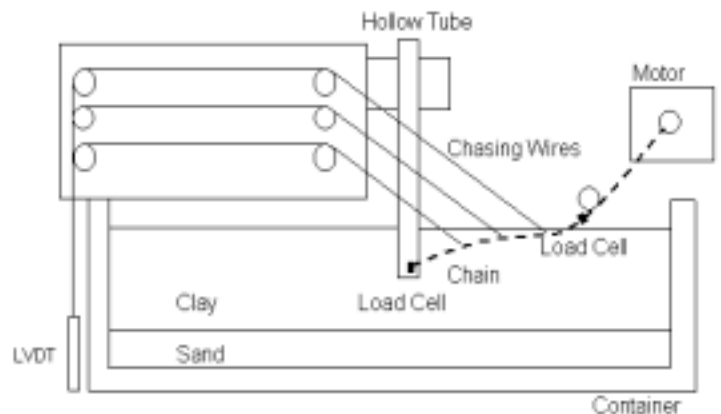


Figure - 1 Centrifuge Test Layout

A centrifuge at the University of Colorado, Boulder, Colorado, was used. It has a capacity of 440 g-tons with a capability of accelerating 2.2 ton payload to a maximum acceleration of 200 g's. It has a radius of 5.49 m from the centrifuge center to the top of the model bucket. The model bucket can be as large as 1.22 m x 1.22 m x 0.91 m.

The soil was first consolidated outside the centrifuge under a constant seepage force and then consolidated further within the centrifuge before the mooring lines were deployed. After the consolidation, the undrained shear strengths of the soil (S_u) were measured in-flight by a miniature vane and correlated with additional

data derived from the void ratio versus shear strength relationship of the test clay (Law, et. al, 1994). The results indicated that S_u remained constant at approximately 3112.2 Pa from the surface to a depth of 3.81 cm and then increased at a rate of 810.57 Pa/cm, indicating higher degrees of overconsolidation near the surface. This corresponds to S_u of 3112.2 Pa from zero to 3.05 m and 1021.06 Pa/m below 3.05 m in the prototype.

After the soil was consolidated, an individual tube with a mooring line attached to its end was inserted vertically into the soil until the mooring line end reached a desired depth. The exposed part of the mooring line above the soil surface was then connected to a step-control motor located at a specified distance away from the tube and pulled under the elevated acceleration within the centrifuge until the line tension reached the specified load.

DESCRIPTION OF ANALYTICAL SOLUTION

The analysis of the static mooring line geometric configuration is based on the limiting equilibrium method in which the detailed solutions are obtained from the static equilibrium conditions. Figure - 2 shows a schematic diagram of a mooring line element embedded in the seafloor. T and ϕ are the axial tensile force and the inclination angle at the ends of the element. N , $(f ds)$, and $(w ds)$ are the normal force, the tangential force, and the buoyant weight of the mooring line element, respectively. From the static equilibrium conditions of forces along the “n” and “t” coordinates and the moment about the point “o”,

$$\begin{aligned} \sum F_t &= 0 \\ \sum F_n &= 0 \\ \sum M &= 0 \end{aligned} \quad (1)$$

unknowns, N , T and ϕ , can be solved. Note that previously published solutions of the embedded mooring line analysis only considered partial equilibrium conditions (Brian Watt Associates, 1983; Degenkamp and Dutta, 1989; Vivatrat, et. al, 1982). The current solution method utilizes complete equilibrium conditions and therefore permits an additional degree of freedom in each mooring line element.

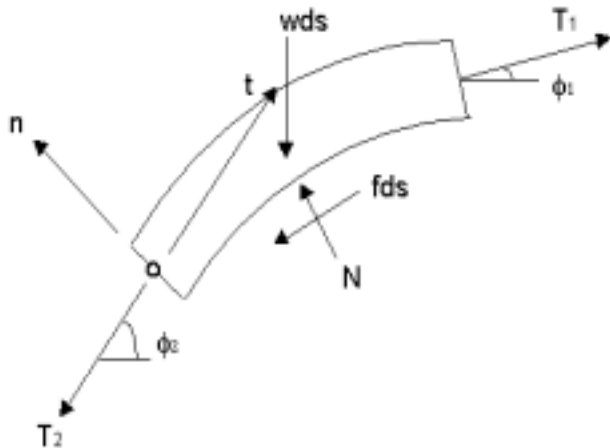


Figure – 2 Mooring Line and Free Body Diagram

In the analysis, it is assumed that the soil tangential forces $(f ds)$ remain at their limiting state at all times, since the dominant mode of the mooring line movement during deployment is sliding. However, the

normal soil forces (N) remain as unknowns because of the available additional degrees of freedom and, therefore, can be less than those defined by the limiting state, i.e., the soil bearing capacity.

Eq. (1) forms the basis of recursion formulas for the detailed analysis of the embedded mooring line element in the seafloor, i.e.,

$$\begin{aligned} T_2 &= T_1 - (f + w \sin \phi_1) ds \\ N &= \frac{2 T_2 - f ds}{\tan \phi_1} \\ \phi_2 &= \phi_1 + \frac{N - w ds \cos \phi_1}{T_2} \end{aligned} \quad (2)$$

where T_1 and T_2 = axial forces at the beginning and end of the element
 ϕ_1 and ϕ_2 = mooring line inclination angle to the horizontal at the beginning and end of the element

f = tangential force per unit length of the element

w = buoyant weight of mooring line per unit length

N = normal force at the bottom of the element.

The solution process starts with a known mooring line inclination angle at the seafloor surface (ϕ_1). The catenary and embedded portions of the mooring line are then solved separately and added for the final solution.

With a known inclination angle at the seafloor surface and the horizontal force at the water surface, the mooring line axial tension at the seafloor surface (T_1) is calculated. Using Eq. (2), the axial tension and the inclination angle at the end of the element, T_2 and ϕ_2 , are then calculated. The calculated orientation angle and the axial force at the end of the previous element become those at the beginning of the new element due to the compatibility requirements. However, when the chasing wire is attached, the orientation angle and the axial force at the beginning of the next element are altered as shown in Figure - 3. Because of the available equilibrium conditions, only two unknowns can be calculated.

The centrifuge test results include the values of the angles θ_c and θ_2 , but not the forces T_c and T_2 . Therefore, the force T_2 can be calculated from the equilibrium of forces at the point of the chasing wire attachment.

Figure - 3 shows a schematic diagram indicating the directions and magnitudes of forces acting at the attachment point. From the equilibrium of forces along the horizontal and vertical directions, the following equations are obtained.

$$\begin{aligned} T_2 \cos \theta_2 + T_c \cos \theta_c &= T_1 \cos \theta_1 \\ T_c \sin \theta_c + T_1 \sin \theta_1 &= T_2 \sin \theta_2 \end{aligned} \quad (3)$$

These equations lead to

$$T_2 = T_1 \frac{\sin(\theta_1 * \theta_c)}{\cos \theta_c * \sin \theta_2} * \frac{\tan \theta_2}{\tan \theta_2 + \tan \theta_c} \quad (4)$$

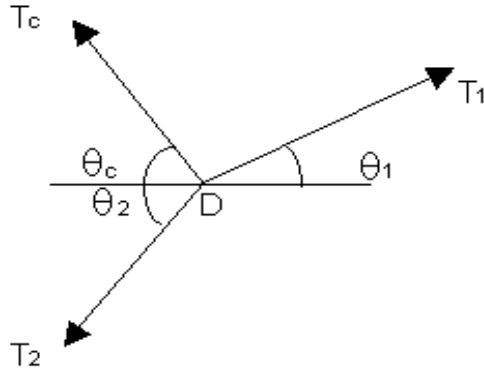
T_2 in Eq. (4) is the adjusted axial force at the end of element considering the effect of the chasing wire.

In the recursion equations, the element tangential force per unit length, f , is estimated assuming that the soil undrained shear strength is fully mobilized, i.e.,

$$f = E_s D \alpha \beta S_u \quad (5)$$

where E_s = equivalent diameter conversion factor for sliding force to

convert mooring line diameter to circumferential area
 D = chain link or cable diameter
 α = soil adhesion conversion factor
 β = contact area conversion factor
 S_u = soil undrained shear strength.



θ_1 = inclination of mooring cable before influenced by chasing wire
 θ_c = inclination of chasing wire
 θ_2 = inclination of mooring cable after influenced by chasing wire
 T_1 = mooring cable force before influenced by chasing wire
 T_c = force in chasing wire
 T_2 = mooring cable force after influenced by chasing wire

Figure - 3 Definition of Angles and Forces

The soil adhesion conversion factor (α) is the ratio of the adhesion between the mooring line and the soil versus the soil cohesion. The contact area conversion factor (β) is the ratio of the true contact area between the mooring line and the soil versus the surface area of a cylinder defined by the mooring line.

The value of the normal force, N , is limited to be no greater than the soil bearing capacity, i.e.,

$$N < N_{\max} = q \, ds$$

$$q = E_b \, D \, S_u \, N_c \quad (6)$$

where q = bearing capacity of soil per unit length

E_b = equivalent diameter conversion factor for normal force to convert mooring line diameter to projected bearing area

N_c = soil bearing capacity factor.

MOORING CABLE VALIDATION STUDY

The following input data were used for the mooring cable validation study. Note that the numbers inside the parenthesis indicate the prototype values, considering the acceleration level of 80 g's used in the centrifuge testing.

Mooring cable diameter = 0.48 cm (38.1 cm)
Diameter factor for cable bearing (E_b) = 1.0
Diameter factor for cable sliding (E_s) = 0.262
Mooring cable tension = 231.3 N (1480.29 kN)
Depth to fixed end = 15.24 cm (12.19 m)
Distance from fixed end to chasing wire attachment
point B = 4.69 cm (3.75 m)
point C = 10.78 cm (8.62 m)
point D = 18.37 cm (14.7 m)

point E = 25.87 cm (20.7 m)
Water depth = 0 (0)
Horizontal distance from fixed end to load application
34.29 cm (27.43 m)
Soil undrained shear strength
3112.2 Pa from 0 ~ 3.81 cm (0 ~ 3.05 m)
810.57 Pa/cm from 3.81 cm (1021.06 Pa/m)

Details of other parameters, such as the inclination angles of the chasing wires and the mooring lines as influenced by the chasing wires, are described in Bang (1998).

To validate the analytical solution, the effects of the following parameters have been studied: the bearing capacity factor for cables (N_{cw}) and the product of the soil adhesion conversion factor for cables (α_w) and the cable contact area conversion factor (β_w). This was because the tangential force developed at the bottom side of the mooring line was influenced by the product of α_w and β_w and no attempt was made to separate the effects of these two parameters during the model test.

Figure - 4 shows the effect of N_{cw} on the mooring cable geometry. Note that the value of $\alpha_w \beta_w$ is 1.0 for all values of N_{cw} . It indicates that the effect of N_{cw} is relatively insignificant for the magnitudes considered ($N_{cw} = 7 \sim 13$). Values of N_{cw} between 7 and 9 provide very good comparisons with the experimental measurement. As the value of N_{cw} increases, the mooring cable profile tends to shift upward.

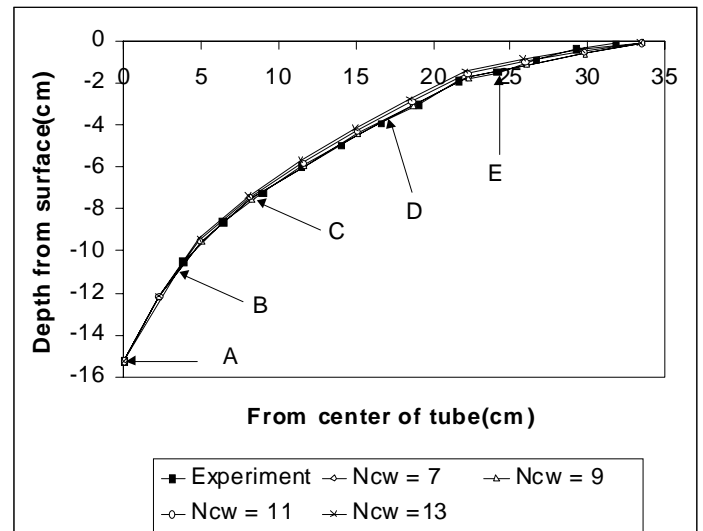


Figure – 4 Mooring Line Geometry with Various Values of N_{cw}
(Test 1-4 : For prototype Dimensions, Multiplied by 80)

Figure - 5 shows the effect of $\alpha_w \beta_w$ on the mooring cable geometry with N_{cw} of 9. The results indicate that the influence of $\alpha_w \beta_w$ is virtually nonexistent when the value of $\alpha_w \beta_w$ varies from 0.5 to 3.2.

Figure - 6 shows the changes in mooring cable forces at the ground surface (T_{surface}) and at the fixed end (T_{anchor}) as a function of $\alpha_w \beta_w$. Note that the measured mooring cable force at the fixed end is 1,170,001.92 N.

Results indicate that the mooring cable geometry as influenced by the chasing wires can be estimated very accurately using the values of $N_{cw} = 7 \sim 9$ and $\alpha_w \beta_w = 0.5 \sim 3.2$. However, the measured mooring cable force at the fixed end is significantly influenced by the values of N_{cw} and $\alpha_w \beta_w$. The measured mooring cable force at the fixed end could be obtained if the values of $\alpha_w \beta_w$ of 3.2 and N_{cw} of 9 are used.

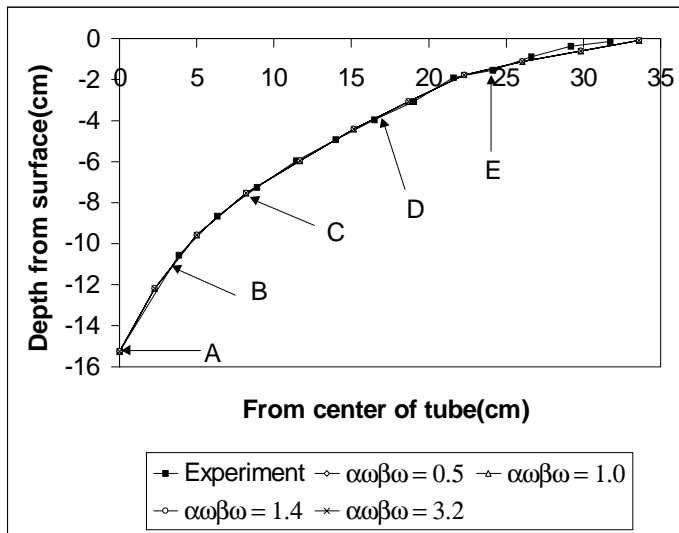


Figure - 5 Mooring Line Geometry with Various Values of $\alpha_w \beta_w$
(Test 1-4 : For prototype Dimensions, Multiplied by 80)

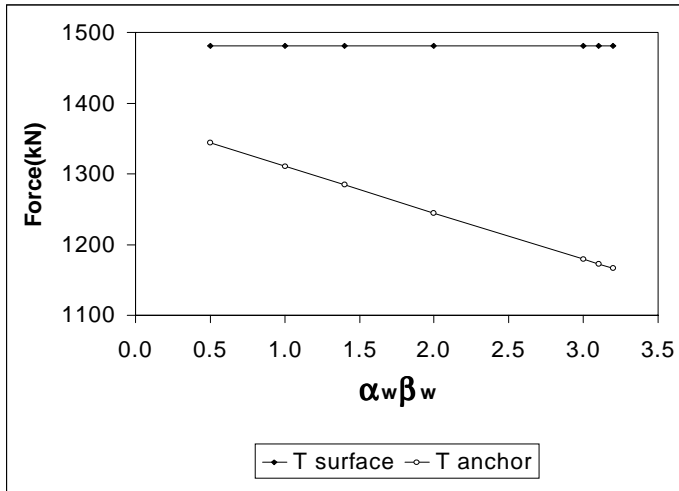


Figure - 6 Mooring Cable Force Variation with $\alpha_w \beta_w$

MOORING CHAIN VALIDATION STUDY

The following input data were used for the mooring chain validation study. The numbers inside the parenthesis indicate the prototype values, considering the acceleration level of 80g's used in the centrifuge testing. Ball chain was used to model the mooring chain.

Ball chain diameter = 0.48 cm
Equivalent mooring chain link diameter = 13.61 cm
Diameter factor for chain bearing (E_b) = 0.233
Diameter factor for chain sliding (E_s) = 0.733
Mooring chain tension = 208.61 N (1,334.4 kN)
Depth to fixed end
5.08 cm (4.06 m) for test 1-1
10.06 cm (8.13 m) for test 1-2
15.24 cm (12.19 m) for test 1-3
Water depth = 0 (0)
Horizontal distance from fixed end to load application

24.13 cm (19.3 m) for test 1-1
31.75 cm (25.4 m) for test 1-2
36.83 cm (29.47 m) for test 1-3
Soil undrained shear strength
3112.2 Pa from 0 ~ 3.81 cm (0 ~ 3.05 m)
810.57 Pa/cm from 3.81 cm (1021.06 Pa/m)

As indicated in the mooring cable analysis, the effects of the soil adhesion conversion factor for chains (α_c) and the chain contact area conversion factor (β_c) were combined.

To narrow down the variations in input parameters, a preliminary analytical parametric study was conducted using the developed solution method. From the preliminary parametric study, it was concluded that the optimum value of the bearing capacity factor for chains (N_{cc}) that matches the mooring line trajectories lies between 13 and 17, and the optimum value of $\alpha_c \beta_c$ lies between 1 and 2. The trajectories tend to shift upward as the value of N_{cc} increases, with virtually no influence from the change in value of $\alpha_c \beta_c$. However, the value of $\alpha_c \beta_c$ has a significant effect on the mooring chain force at the fixed end. In general, as the value of $\alpha_c \beta_c$ increases, the force at the fixed end decreases.

To determine the optimum value of $\alpha_c \beta_c$, second vector norms of error in $\alpha_c \beta_c$ were calculated for various N_{cc} values and they were used to calculate the optimum values of $\alpha_c \beta_c$ at given N_{cc} , as shown in Table - 1. A linear regression analysis with a second order polynomial indicated that the value of $\alpha_c \beta_c$ of 1.45 produced the optimum value.

N_{cc}	$\alpha_c \beta_c$
13	1.448
14	1.445
15	1.451
16	1.444
17	1.441
$\alpha_c \beta_c$, ave.	= 1.45

Table - 1 Optimum Values of $\alpha_c \beta_c$

To study the effect of the value of N_{cc} on the mooring chain geometry, the trajectory of each mooring line was compared with predictions with various values of N_{cc} varying from 13 to 17 but with the fixed, optimum value of $\alpha_c \beta_c$ of 1.45. One such example is shown in Figure - 7, which compares the measured mooring chain trajectory of Test 1 - 3 of those calculated with various values of N_{cc} . The effect of N_{cc} on the mooring chain trajectory is clearly observed from the figure. The mooring chain trajectory shifts upward as the value of N_{cc} increases. Overall, the value of N_{cc} of 14 produces the best results when all test results are considered.

Table - 2 shows the comparisons of measured and calculated mooring chain forces at the fixed end (T_{anchor}). $\alpha_c \beta_c$ value remained as 1.45, since it was determined to be the optimum value. As can be seen from Table - 2, it is apparent that the force at the fixed end is not influenced much by the value of N_{cc} .

Results indicate that the mooring chain trajectory is primarily influenced by the value of N_{cc} , whereas the force at the fixed end is primarily influenced by the value of $\alpha_c \beta_c$. The mooring chain geometry and the force at the fixed end as influenced by the chasing wires can be estimated with reasonable accuracy using the values of $N_{cc} = 14$ and $\alpha_c \beta_c = 1.45$.

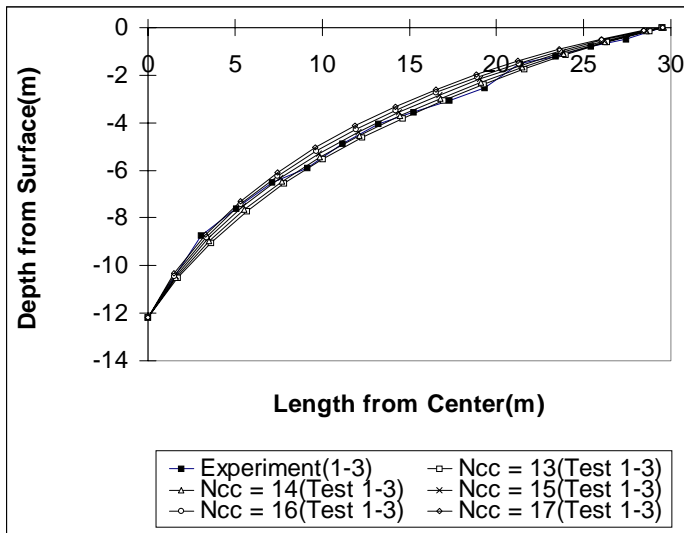


Figure – 7 Mooring Line Geometry of Test 1-3 with N_{cc} Variation ($\alpha_c \beta_c = 1.45$)

Test No.	T_{test} (kN)	N_{cc}	T_{anchor} (kN)	Error
Test 1-1	1107.37	13	1219.1	-0.101
		14	1218.21	-0.100
		15	1217.39	-0.099
		16	1215.43	-0.098
		17	1214.82	-0.097
Test 1-2	886.47	13	1126.94	-0.271
		14	1123.44	-0.267
		15	1123.18	-0.267
		16	1121.6	-0.265
		17	1120.22	-0.264
Test 1-3	1043.89	13	1005.86	0.036
		14	1003.69	0.039
		15	1003.3	0.039
		16	1003.03	0.039
		17	1002.9	0.039

Table - 2 Comparisons of Measured and Calculated Forces at Anchor ($\alpha_c \beta_c = 1.45$)

CONCLUSION

From the results of the validation study, the optimum values of N_c and $\alpha \beta$ have been determined as follows.

For mooring cable, $N_{cw} = 9$

$$\alpha_w \beta_w = 3.2$$

For mooring chains, $N_{cc} = 14$

$$\alpha_c \beta_c = 1.45$$

The optimum value of N_c for the mooring cable is very close to that predicted by conventional foundation bearing capacity theories, whereas the optimum value of N_c for mooring chains is higher. The reason is not perfectly clear and needs to be studied in detail in the future.

It is noted that $N_{cc} = 13$ and $\alpha_c \beta_c = 1.4$ were obtained in the previous study (Bang, et.al, 1996) which did not consider the effect of chasing wires on mooring chains. Although the differences in values of N_{cc} and $\alpha_c \beta_c$ are noted with and without considering the effect of chasing wires, the difference is not significant for mooring chains. However, the effect of chasing wires is significant on mooring cables. In future centrifuge tests, better instrumentation technique of locating the mooring line geometry should be used to eliminate completely the effect of chasing wires.

It is noted that these values have been determined from comparisons with the centrifuge test results on mooring lines with chasing wires. Therefore, the use of these values for mooring lines with no chasing wires may not be applicable.

ACKNOWLEDGMENTS

The authors are grateful to the technical and financial supports provided by the U.S. office of Naval Research and the Naval Facilities Engineering Service Center. The work has been supported by the Department of the Navy, Office of Naval Research, grant number N00014 - 97 - 1 - 0887. The content of this paper does not necessarily reflect the position or the policy of the U.S. Government.

REFERENCES

- Bang, S (1996). "Anchor Mooring Line Computer Program User Manual," Contract Report CR - 6020 - OCN, Naval Facilities Engineering Service Center.
- Bang, S (1998) "Use of Suction Piles for Mooring Of mobile Offshore Bases," Quarterly Progress Report prepared for Naval Facilities Engineering Service Center.
- Bang, S, and Taylor, RJ, Jie, Y, and Kim, HT (1996). "Analysis of Anchor Mooring Line in Cohesive Seafloor," Transportation Research Record, No. 1526.
- Brian Watt Associates, Inc (1983). "A Method for Predicting Drag Anchor Holding Capacity," Report No. CR 83.036.
- Degenkamp, G, and Dutta, A (1989). "Soil Resistance to Embedded Anchor Chain in Soft Clay," *Journal of Geotechnical Engineering*, Vol. 115, No. 19.
- Dunnavant, TW, and Kwan, CTT (1993). "Centrifuge Modeling and Parametric Analysis of Drag Anchor Behavior," *Offshore Technology Conference Paper No. 7202*.
- Law, HK, et. al (1994). "Centrifuge Testing for Dynamic Anchor Line Modeling," A Report submitted to Naval Facilities Engineering Service Center, Univ. of Colorado, Boulder.
- Vivatrat, V, Valent, PJ, and Ponterio, AA (1982). "The Influence of Chain Friction on Anchor Pile design," *Proc., 14th Annual Offshore Technology Conference*, Paper No. 4178.